Graphene Oxide–Assisted Dispersion of Pristine Multiwalled Carbon Nanotubes in Aqueous Media

ARTICLE *in* THE JOURNAL OF PHYSICAL CHEMISTRY C · JULY 2010

Impact Factor: 4.77 · DOI: 10.1021/jp103745g

4 AUTHORS, INCLUDING:

Chao Zhang
Donghua University
43 PUBLICATIONS **1,067** CITATIONS
SEE PROFILE

Tianxi Liu
Fudan University
233 PUBLICATIONS **7,181** CITATIONS
SEE PROFILE

Graphene Oxide-Assisted Dispersion of Pristine Multiwalled Carbon Nanotubes in Aqueous Media

Chao Zhang, Lulu Ren, Xiaoyan Wang, and Tianxi Liu*

Key Laboratory of Molecular Engineering of Polymers of Ministry of Education, Department of Macromolecular Science, Laboratory of Advanced Materials, Fudan University, 220 Handan Road, Shanghai 200433, People's Republic of China

Received: April 26, 2010; Revised Manuscript Received: May 22, 2010

Graphene oxide (GO) sheets, considered as "soft" two-dimensional macromolecules containing multiple aromatic regions and hydrophilic oxygen groups, can adsorb the pristine multiwalled carbon nanotubes (MWNTs) through the π-stacking interaction, thus causing pristine MWNTs to stably disperse and fractionate in aqueous media. The water-soluble and insoluble complexes can be obtained by changing the initial proportion of MWNTs to GO sheets, which are important for noncovalent approaches toward solubilizing CNTs and open a new way for GO applications in colloidal chemistry. Solubility results indicate that the GO sheets are prone to stabilize MWNTs with larger diameters. When the diameters of CNTs decrease to a critical value, the π-stacking interactions are weakened by large surface energy among CNTs themselves; the CNTs are inclined to form bundles or twisted structures instead of CNT−GO complexes. This can be probably developed into a practical method to fractionate MWNTs with different outer diameters in water.

1. Introduction

In the past decade, carbon nanotubes (CNTs) have attracted considerable attention due to their unique nanostructures and excellent physical properties.[1−4] The inherent insolubility of pristine CNTs in solvents, particularly in water, however, has complicated their uses and processing in composites and thus greatly limited their integration in potential biomedical applications and biophysical processing schemes.[5−8] Thus, CNTs have to be dispersed in organic or aqueous solvents before solution-phase processing, separation, and assembly can be practical methods. In recent years, several studies have focused on the solubility of other nanomaterials such as carbon black,[9,10] fullerene,[11−13] and nanocrystals.[14−17] Similarly, much effort has been made toward solubilizing CNTs in aqueous media by engineering the CNT surfaces through either covalent[18−26] or noncovalent[27−33] approaches. For covalent functionalization, the instrinsic electrical and thermal conductivity properties of CNTs are often severely impaired. Hence, the noncovalent functionalization of CNTs is particularly attractive because it offers the possibility of attaching chemical handles without affecting the electronic network of the tubes. In noncovalent approaches, dissolution of CNTs in water, based on van der Waals forces or π-stacking interactions, has been facilitated by surfactants and polymer wrapping. However, the use of surfactants may largely affect the properties of the prepared composites and their further uses. Also, the number of polymers used for polymer-based solubilization of CNTs is limited. Therefore, seeking proper materials to form complexes with CNTs, by stabilizing CNTs in water and endowing CNTs with additional performance, has become a new challenge for noncovalent approaches toward solubilizing CNTs.

Recently, graphene, a novel one-atom-thick two-dimensional graphitic carbon material, has also attracted tremendous attention because of its extraordinary electronic,[34−38] thermal,[39] and mechanical properties[40−42] and thus has many potential and promising applications.[43] Graphite oxide, consisting of two-dimensional oxidized graphene sheets, can be readily exfoliated into individual graphene oxide (GO) sheets to yield stable suspensions in water because of the hydrophilic oxygen groups attached to the strongly oxygenated graphene sheets.[44−46] Herein, we report a noncovalent and nonorganic strategy for stabilizing aqueous dispersions of high weight fraction CNTs with the addition of GO sheets. A simple solubilization strategy for dramatically reducing the CNT breakage is developed, in which the pristine CNTs are mixed with GO sheets using low-power, high-frequency sonicators for a certain time. Most interestingly, this solubilization approach for CNTs is found to be tube size specific, suggesting that this can be probably developed into a practical method to fractionate MWNTs with different outer diameters in water.

2. Experimental Methods

2.1. Materials. Natural graphite powder was purchased from Alfa Aesar and used without further purification. Ultrapure Milli-Q water was used throughout all of the experiments. SWNTs (length, 5−30 μm; outer diameter (OD), 1−2 nm; purity, 90%) and MWNTs (length, 10−30 μm; outer diameter, 40−50 nm, 20−30 nm, <8 nm, respectively; purity, 95%), produced by the CVD method, were supplied by Chengdu Institute of Organic Chemistry, Chinese Academy of Sciences, China. All of the other reagents were purchased from Sinopharm Chemical Reagent Co. Ltd. and used as received.

2.2. Preparation and Purification of Graphite Oxide. Graphite oxide was synthesized by the Hummers method. In a typical process, a mixture of graphite (2.50 g) and $NaNO_3$ (5.00 g) was placed in cold (0 °C) concentrated H_2SO_4. An amount of 7.50 g of $KMnO_4$ was added gradually with stirring and cooling, so that the temperature of the mixture was not allowed to reach 20 °C. The mixture was then maintained at 35 ± 3 °C for 30 min. After that, deionized water (230 mL) was slowly added to the mixture, and the temperature was increased to 98

* To whom correspondence should be addressed. Tel.: +86-21-55664197. Fax: +86-21-65640293. E-mail: txliu@fudan.edu.cn.

10.1021/jp103745g
Published on Web 06/15/2010

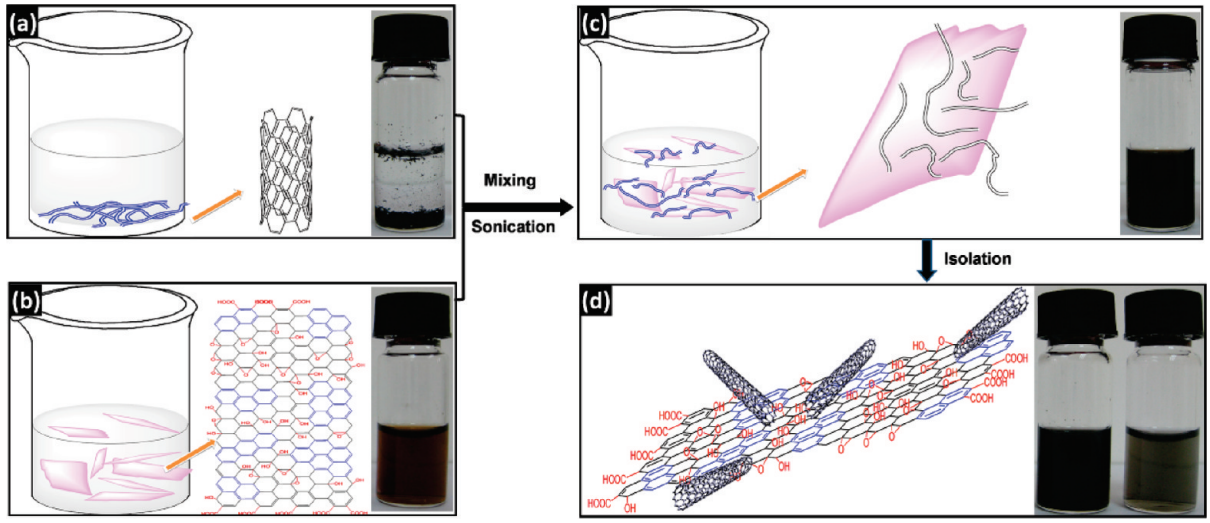

Figure 1. Schematic mechanism for formation of the MWNT−GO complexes.

°C. After 15 min, the mixture was further treated with 350 mL of deionized water and 25 mL of 5% H_2O_2 solution, and then filtered and washed successively with 10% HCl aqueous solution completely until sulfate could not be detected with $BaCl_2$. The resulting solid filtration residue was suspended in water under ultrasonication for 0.5 h, followed by centrifugation at 4000 rpm (2770*g*) for 0.5 h. The obtained supernate was dried via evaporation of water under vacuum.

2.3. Preparation of Multiwalled Carbon Nanotube−Graphene Oxide Complexes (MWNT−GO Complexes). Graphite oxide was dispersed in water (1.0 mg mL^{-1}) by ultrasonication for 1 h at a power of 135 W and centrifuging at 14 000 rpm (17 530*g*) for 20 min to further remove aggregates. The obtained supernates were used to disperse MWNTs throughout all of the experiments. The aqueous colloidal suspensions of GO sheets were then poured into the MWNT conglomerations, and the mixture was then sonicated for 1 h at 45 W. This suspension was centrifuged for 30 min at 8000 rpm (8860*g*) to remove the unstabilized MWNTs, thus giving a suspension of the MWNT−GO complexes and the excess GO sheets in the supernatant. Next, the MWNT−GO complexes were separated from the excess GO sheets by repeating centrifugation (14 000 rpm, 17 530*g*, 20 min) and water washing steps.

2.4. Characterizations. Transmission electron microscopy (TEM) observations were performed under an acceleration voltage of 200 kV with a Philips CM 300 FEG TEM. AFM images were taken in tapping mode with a scanning probe microscope (SPM) Nanoscope IV from Digital Instruments. UV−vis spectra were recorded on a Lambda 35 Perkin-Elmer spectrometer. The emission spectra were recorded on a Shimadzu RF-5301 PC fluorometer at room temperature. The FTIR spectra were recorded with a 4 cm^{-1} spectral resolution on a Nicolet Nexus 470 spectrometer equipped with a DTGS detector by signal averaging 64 scans.

3. Results and Discussion

In the present study, we prepared MWNT−GO complexes as illustrated in Figure 1. It can be seen that the pristine MWNTs cannot form stable suspensions in water even after a long time ultrasonication, thus leading to serious precipitation and strong aggregation (Figure 1a). The suspensions of GO sheets used here were the highly stable supernatants by centrifuging at 13 500 rpm (16 300*g*) for 20 min. Figure S1 showed the TEM image at low magnification for the GO sheets, which tend to congregate together to form multilayer agglomerates. Some individual nanosheets can also be observed, having dimensions of several hundred to several thousand nanometers. The morphology of the exfoliated GO sheets was further examined by tapping-mode AFM. Figure S2 showed individually dispersed two-dimensional ultrathin nanosheets with lateral dimensions of up to 3 μm, although some large nanosheets with lateral dimensions of >3 μm were occasionally observed. The GO sheets deposited on mica substrate were morphologically irregular and dimensionally largely diminished as compared to the natural graphite crystals, indicating the breakage or fracture of sheets during the oxygenation and ultrasonication process. The height profile in Figure S2 revealed that the nanosheets had an average thickness of about 1.0 nm. This value indicated the successful exfoliation, and the unilamellar GO sheets were obtained. On the basis of TEM and AFM studies on the GO sheets collected from the supernatants, it was observed that sonication results in nearly complete exfoliation of the GO into single sheet. Because of the presence of hydrophilic groups such as hydroxyl, epoxy, and carboxyl groups on the GO surfaces and edges, GO sheets formed a brown yellow and stable dispersion in water (Figure 1b). When the aqueous colloidal suspensions of GO sheets were poured into the MWNT conglomerations, the mixture was then sonicated for 1 h at 45 W. The brown yellow dispersion turned black, suggesting some MWNTs come into the upper supernatant, as shown in Figure 1c. The suspension can be thought of as a mixture of MWNT−GO complexes, excess GO sheets, and unstabilized MWNTs. This suspension was centrifuged for 30 min at 8000 rpm (8860*g*) to remove the unstabilized MWNTs, thus giving a suspension of the MWNT−GO complexes and the excess GO sheets in the supernatant. Next, the MWNT−GO complexes were separated from the excess GO sheets by repeating centrifugation (14 000 rpm, 17 300*g*, 20 min) and water washing steps. Figure 1d showed the MWNT−GO complexes after being redispersed and diluted in water. The black dispersion of MWNT−GO complexes is very stable at room temperature without any precipitation upon storage for weeks, indicating strong stabilizing ability of the GO sheets for the pristine MWNTs in water. It is reasonable to suppose that the π-conjugated multiple aromatic regions (marked in blue in Figure 1d) of GO sheets could interact with the sidewalls of MWNTs through the π-stacking interaction, while the hydrophilic oxygen

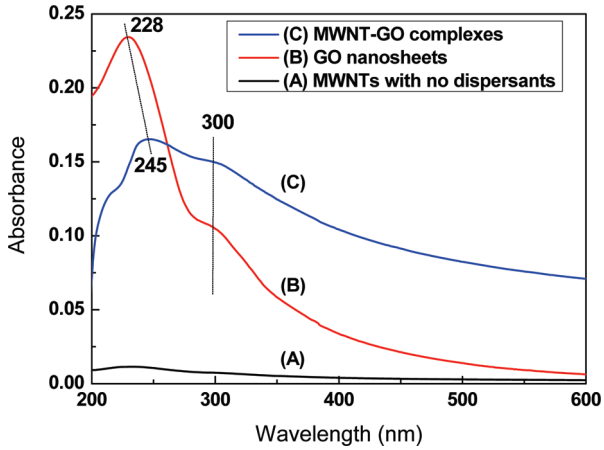

Figure 2. UV−vis absorption spectra of the supernatant of (A) MWNTs without dispersants; (B) the GO sheets; and (C) the MWNT−GO complexes.

groups (marked in red in Figure 1d) maintain the water solubility of the MWNT−GO complexes.

The UV−vis spectra of the supernatants of MWNT−GO complexes are shown in Figure 2. The spectra were recorded using the supernatant of MWNTs without the dispersants, GO sheets, and MWNT−GO complexes. The supernatants were diluted in the same ratio before measurement. It is widely accepted that the absorption intensity is proportional to the concentration of CNTs dissolved in the suspension. The supernatant of MWNTs with no dispersants indicates no obvious peaks in the measured scale, indicating that almost all of the MWNTs precipitated after centrifugation. The GO sheets demonstrate an absorption peak centered at 228 nm and a shoulder peak at about 300 nm, which could be assigned to the $\pi \rightarrow \pi$ transitions of aromatic C−C bonds and the $n \rightarrow \pi$ transitions of C═O bonds, respectively. These peak positions agree well with those reported by many other studies. After MWNTs were added and isolated by repeating sonication−centrifugation cycles, MWNT−GO complexes were redispersed into water and recorded in the spectra. With the addition of GO sheets, the absorption peaks in the visible region agree well with the reported spectra of CNT mixtures, indicating that the MWNTs can be effectively stabilized by the GO sheets in the supernatant. As compared to the spectra of GO sheets, the shoulder peak of MWNT−GO complexes at about 300 nm does not shift, indicating that the $n \rightarrow \pi$ transitions of C═O bonds of GO sheets were not affected by the addition of MWNTs. The bathochromic shift of the absorption peak centered at 228 nm shifting to about 245 nm confirms the formation of MWNT−GO complexes via the π-stacking interactions of the multiple aromatic regions of GO sheets and the sidewalls of the MWNTs.[47−49]

Emission spectra of the supernatant of GO sheets and MWNT−GO complexes were collected to study the photoluminescence property of the MWNT−GO complexes. Figure 3a showed the emission spectra of the supernatant of GO sheets and MWNT−GO complexes, with the excitation wavelength set to $\lambda_{max} = 350$ nm for each sample. GO sheets are strongly luminescent, showing a broad absorption band centered at ~580 nm, as illustrated by the emission spectrum in Figure 3a (being excited at 350 nm). As we know, the supernatant of the pristine MWNTs yields no emission at this excitation wavelength, while the MWNT−GO complexes also display slightly quenched fluorescence as seen from the emission spectrum of the MWNT−GO complexes (also being excited at 350 nm). Figure 3b shows the emission spectra of MWNT−GO complexes

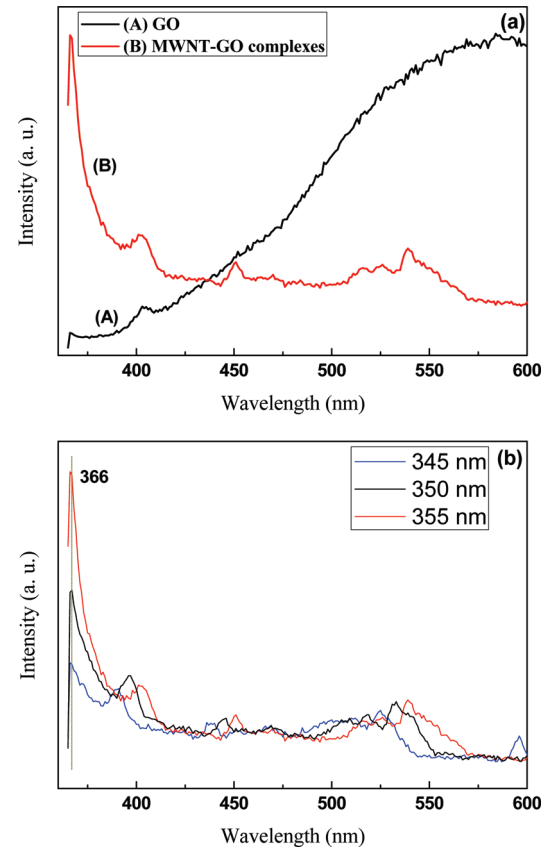

Figure 3. (a) Emission spectra of the supernatant of GO sheets and MWNT−GO complexes, with the excitation wavelength set to $\lambda_{max} =$ 350 nm for each sample. (b) Emission spectra of MWNT−GO complexes excited at 345, 350, and 355 nm.

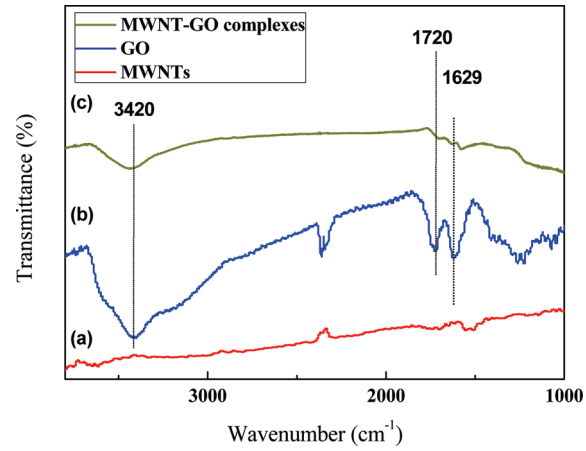

Figure 4. FTIR spectra of (A) the MWNTs; (B) the GO sheets; and (C) the MWNT−GO complexes.

excited at 345, 350, and 355 nm, indicating that the sharp and intense peaks (~366 nm for emission spectrum) are the Raman peaks of water and the multiplets between 380 and 550 nm are assigned to the scattering peaks. It was surprisingly found that the excited states of GO sheets are significantly quenched when the MWNTs were physically adsorbed on the GO planes. Such a phenomenon has never been reported before.

In Figure 4, FTIR spectra of pristine MWNTs, GO sheets, and MWNT−GO complexes provided additional information on the successful manufacture of composition by confirming the existence of GO sheets in MWNT−GO complexes. The FTIR spectrum of the GO sheets (curve B) shows a broad absorption band at 3410 cm^{-1}, which is assigned to the OH

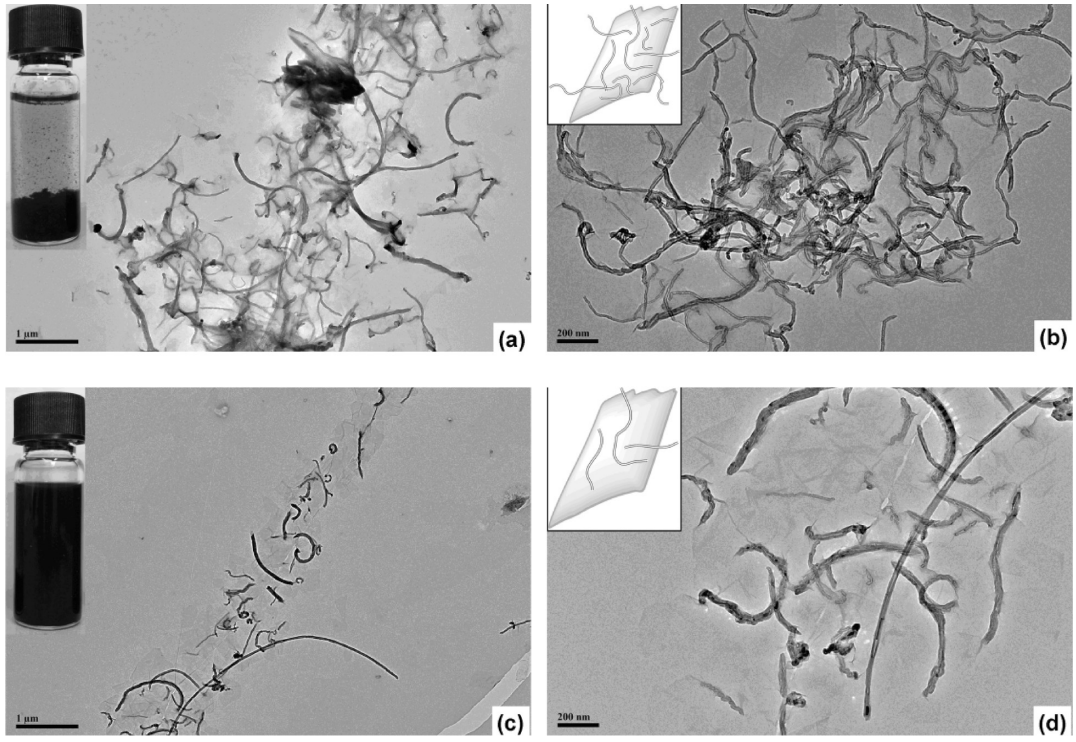

Figure 5. TEM images of interactions formed between MWNTs and GO sheets by changing the initial proportion of MWNTs to GO sheets with 2:1 at different magnifications (a,b) and the initial proportion of MWNTs to GO sheets with 1:2 at different magnifications (c,d). The inset in (b,d) is the schematic description of the MWNT−GO complexes.

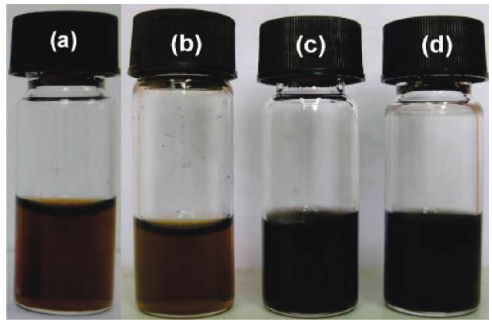

Figure 6. Digital pictures showing the supernatants of mixtures of (a) SWNTs (OD: 0.8−1.3 nm), (b) MWNTs (OD: <8 nm), (c) MWNTs (OD: 20−30 nm), and (d) MWNTs (OD: 40−50 nm) after sonication. These dispersions were centrifuged for 30 min at 8000 rpm (8860*g*) to give the supernatants.

groups. Also, the absorption bands at 1629 and 1720 cm^{-1} indicate the presence of carbonyl stretching vibration; that is, the carbonyl and carboxyl groups are bounded to the edges of the basal planes of GO. In the FTIR spectra of the MWNT−GO complex powders (curve C), the broad absorption band from the OH groups and the absorption peak at 1629 and 1720 cm^{-1} from the carbonyl and carboxyl groups are present. These oxygen-containing functional groups are abundant on the GO sheets but do not appear in the spectrum of pristine MWNTs (curve A), which can provide numerous adsorption sites and thus further confirm the existence of GO sheets in the MWNT−GO complexes.

Furthermore, we studied the interactions formed between MWNTs and GO sheets by changing the initial proportion of MWNTs to GO sheets. Direct evidence for the adsorption of the MWNTs on the GO sheet planes and the interaction mechanism can be strongly supported by TEM observation. As shown in Figure 5a, when the initial proportion of MWNTs to GO sheets was 2:1, the single GO sheet with lots of conjugated clusters prefers to interact with the MWNTs around the single sheet in liquid, resulting in the formation of MWNT-coated exfoliated GO sheets. Excessive MWNTs on a single GO sheet and the tubule twist of CNTs fixed on different GO sheets may reduce the solubility of MWNT−GO complexes, thus leading to serious aggregations of MWNT−GO complexes. Even after sonicating these sediments for several minutes, the precipitations composed of all of the initially added MWNTs and GO sheets still remain at the bottom, as shown in the inset picture of Figure 5a. In agreement with the above analysis, we found that in TEM micrographs, the single GO sheets were bestrewed with a great deal of MWNTs (Figure 5b). However, when the initial proportion of MWNTs to GO sheets was 1:2, as shown in Figure 5c, the single GO sheet could still possibly interact with many MWNTs at the beginning. After a dynamic equilibrium process due to long-time sonication, a stable dispersion of MWNT−GO complexes was formed; a proper proportion of MWNTs to GO sheets for individual MWNT-coated exfoliated GO sheets stays stably in the supernatant (the inset picture in Figure 5c). As can be cearly seen by using TEM, a small quantity of hair-like MWNTs were randomly adsorbed on the smooth surface of GO sheets, as shown in Figure 5d, thus forming the water-suspendable MWNT−GO complexes. Therefore, the morphological observations further indicate that the MWNTs were indeed adsorbed onto the GO sheet planes.

For a system containing GO sheets and pristine MWNTs, we are inclined to propose a mechanism that the MWNTs may be adsorbed onto the GO sheet planes or wrapped by GO sheets, primarily depending on the curvature of GO sheets. GO sheets, due to their less perfect crystal structure, are expected to have weaker lattice stretching and bending stiffness than graphene.[50] Therefore, there is much less possibility for the GO to change their conformation into nanotubes or nanoscrolls for wrapping the MWNTs, thus probably revealing the facts that the MWNTs

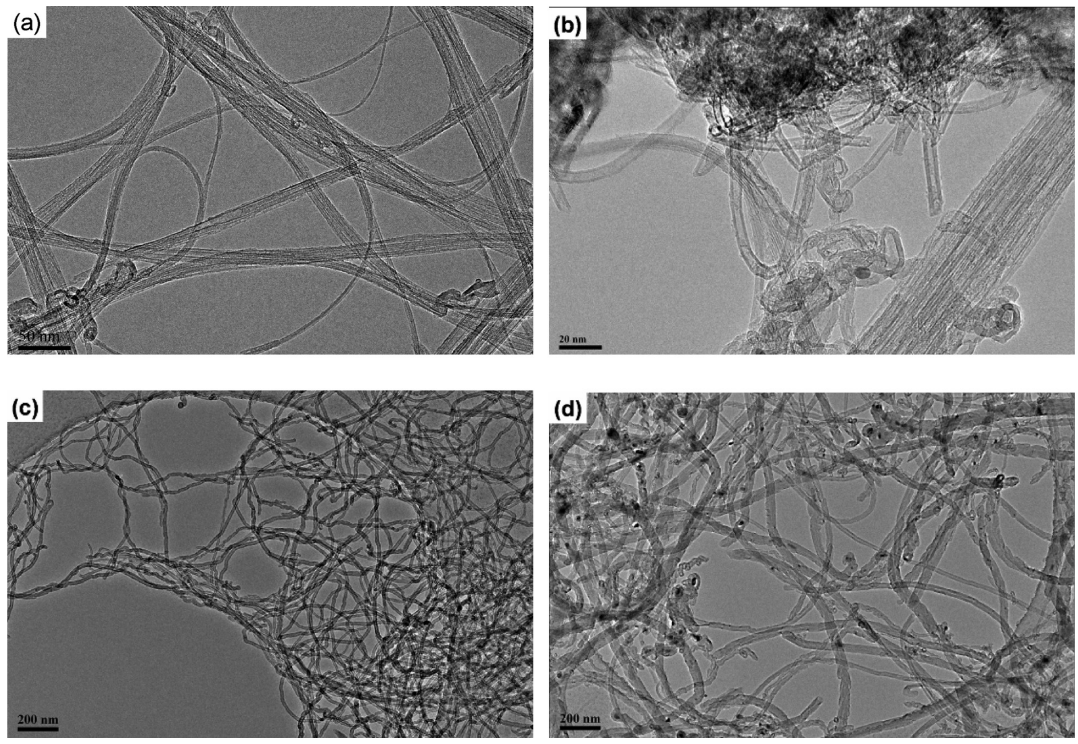

Figure 7. TEM images of (a) SWNTs (OD: 1.0−2.0 nm), (b) MWNTs (OD: <8 nm), (c) MWNTs (OD: 20−30 nm), and (d) MWNTs (OD: 40−50 nm).

were stabilized in liquid through the absorption onto GO sheets instead of being wrapped by GO sheets.

To further study the MWNT dispersion property in GO sheet suspensions and the related mechanism, the GO sheet stabilizing effect for the MWNTs with different outer diameters for the MWNT−GO complexes was investigated. Whether GO sheets can assist in dispersing single-walled carbon nanotubes (SWNTs) was also studied. The resulting mixture suspensions of GO sheets and different diameter CNTs were centrifuged for 30 min at 8000 rpm (8860*g*) to give the supernatants as shown in Figure 6. The color change from brown yellow to black for the supernatants can prove the formation of CNT−GO complexes. When the GO sheet suspensions were mixed with CNTs with different ODs followed by sonicating, the color change was studied by measuring the UV−vis absorption spectra of the supernatants of as-prepared mixtures (as shown in Figure S3). Interestingly, the GO sheets seem to not be able to disperse the MWNTs with diameters less than 8 nm and the SWNTs by such $\pi-\pi$ stacking interactions, indicating a selective adsorption of the GO for the CNTs. As is known, the van der Waals interaction between CNTs mainly depends on the tube diameter. Because of the very large specific surface areas, the SWNTs and smaller MWNTs are seldomly obtained individually but most often in bundle or rope forms.[51] When the diameters of CNTs decrease to a critical value, interestingly, the π-stacking interactions were affected and weakened by large surface energy among CNTs themselves; the CNTs are inclined to form bundles or twisted structures instead of CNT−GO complexes. Direct evidence for the formation of the buddles or twisted structures of the CNTs can be further comfirmed by TEM observation. Figure 7 showed the TEM images of the pristine SWNTs and the MWNTs with outer diameters of less than 8, 20−30, and 40−50 nm, respectively. It can be clearly seen that the SWNTs and the MWNTs with diameters less than 8 nm were arranged into bundles, whereas the MWNTs with larger outer diameters may exist in individual nanotubes. This fact further indicates that the π-stacking interactions between the GO sheets and the pristine MWNTs induce such physical adsorption, and the stacking interaction is not strong enough to overcome the enhanced graphitic intertube interaction of the CNTs with diameters less than 8 nm to form the CNT−GO complexes.

4. Conclusions

In summary, we have found that the GO sheets consisting of multiple aromatic regions and hydrophilic oxygen groups can enhance the stability of pristine MWNTs in water. Solubility results indicate that the GO sheets lean to stabilizing MWNTs with larger diameters, mainly depending on whether the CNTs are inclined to form bundles, twisted structures, or CNT−GO complexes. The MWNT−GO complexes prepared by mild sonication and separation through simple sonicating and centrifugation have good solubility in water, showing potential applications in biomedicine and functional nanocomposites, also opening a new way for the GO applications in colloidal chemistry.

Acknowledgment. We are grateful for the financial support from the National Natural Science Foundation of China (20774019; 50873027), the "Shu Guang" project (09SG02) supported by the Shanghai Municipal Education Commission and the Shanghai Education Development Foundation, and the Shanghai Leading Academic Discipline Project (Project Number: B113).

Supporting Information Available: TEM image of GO sheets at low magnification. Tapping-mode AFM image of the exfoliated GO sheets deposited on a fresh mica substrate. UV−vis absorption spectra of the supernatants of GO sheet suspensions mixed with SWNTs (OD: 0.8−1.3 nm), MWNTs (OD: <8 nm), MWNTs (OD: 20−30 nm), and MWNTs (OD: 40−50 nm). This material is available free of charge via the Internet at http://pubs.acs.org.

References and Notes

(1) Ijima, S. *Nature* **1991**, *354*, 56–58.
(2) Baughman, R. H.; Zakhidov, A. A.; De Heer, W. A. *Science* **2002**, *297*, 787–792.
(3) Kovtyukhova, N. I.; Mallouk, T. E.; Pan, L.; Dickey, E. C. *J. Am. Chem. Soc.* **2003**, *125*, 9761–9769.
(4) Dai, H. *Acc. Chem. Res.* **2002**, *35*, 1035. Sun, Y. P.; Fu, K.; Lin, Y.; Huang, W. *Acc. Chem. Res.* **2002**, *35*, 1096–1104.
(5) O'Connell, M. J.; Bachilo, S. M.; Huffman, C. B.; Moore, V. C.; Strano, M. S.; Haroz, E. H.; Rialon, K. L.; Boul, P. J.; Noon, W. H.; Kittrell, C.; Ma, J. P.; Hauge, R. H.; Weisman, R. B.; Smalley, R. E. *Science* **2002**, *297*, 593–596.
(6) Richard, C.; Balavoine, F.; Schultz, P.; Ebbesen, T. W.; Mioskowski, C. *Science* **2003**, *300*, 775–778.
(7) Dieckmannm, G. R.; Dalton, A. B.; Johnson, P. A.; Razal, J.; Chen, J.; Giordano, G. M.; Munoz, E.; Musselman, I. H.; Baughman, R. H.; Draper, R. K. *J. Am. Chem. Soc.* **2003**, *125*, 1770–1777.
(8) Zheng, M.; Jagota, A.; Semke, E. D.; Diner, B. A.; McLean, R. S.; Lustig, S. R.; Richardson, R. E.; Tassi, N. G. *Nat. Mater.* **2003**, *2*, 338–342.
(9) Watt, J. D.; Franklin, R. E. *Nature* **1957**, *180*, 1190–1194.
(10) Thomas, W. J. *Carbon* **1966**, *3*, 435–443.
(11) Deguchi, S.; Alargova, R. G.; Tsujii, K. *Langmuir* **2001**, *17*, 6013–6017.
(12) Nakamura, E.; Isobe, H. *Acc. Chem. Res.* **2003**, *36*, 807–815.
(13) Kokubo, K.; Matsubayashi, K.; Tategaki, H.; Takada, H.; Oshima, T. *ACS Nano* **2008**, *2*, 327–333.
(14) Connolly, S.; Fitzmaurice, D. *Adv. Mater.* **1999**, *11*, 1202–1205.
(15) Aldana, J.; Wang, Y. A.; Peng, X. G. *J. Am. Chem. Soc.* **2001**, *123*, 8844–8850.
(16) Zhuang, J. Q.; Zhang, X. D.; Wang, G.; Li, D. M.; Yang, W. S.; Li, T. J. *J. Mater. Chem.* **2003**, *13*, 1853–1857.
(17) Fan, H. Y. *Chem. Commun.* **2008**, *12*, 1383–1394.
(18) Sun, Y.-P.; Huang, W.; Lin, Y.; Fu, K.; Kitaygorodskiy, A.; Riddle, L. A.; Yu, Y. J.; Carroll, D. L. *Chem. Mater.* **2001**, *13*, 2864–2869.
(19) Pan, H. L.; Liu, L. Q.; Guo, Z. X.; Dai, L. M.; Zhang, F. S.; Zhu, D. B.; Czerw, R.; Carroll, D. L. *Nano Lett.* **2003**, *3*, 29–32.
(20) Stevens, J. L.; Huang, A. Y.; Peng, H.; Chiang, I. W.; Khabashesku, V. N.; Margrave, J. L. *Nano Lett.* **2003**, *3*, 331–336.
(21) Bianco, A.; Prato, M. *Adv. Mater.* **2003**, *15*, 1765–1768.
(22) Fernando, K. A. S.; Lin, Y.; Sun, Y. P. *Langmuir* **2004**, *20*, 4777–4778.
(23) Qin, S.; Qin, D.; Ford, W. T.; Herrera, J. T.; Resasco, D. E.; Bachilo, S. M.; Weisman, R. B. *Macromolecules* **2004**, *37*, 3965–3967.
(24) Tagmatarchis, N.; Zattoni, A.; Reschilian, P.; Prato, M. *Carbon* **2005**, *43*, 1984–1989.
(25) Chen, S.; Shen, W.; Wu, G.; Chen, D.; Jiang, M. *Chem. Phys. Lett.* **2005**, *402*, 312–317.
(26) Yang, D.; Guo, G. Q.; Hu, J. H.; Wang, C. C.; Jiang, D. L. *J. Mater. Chem.* **2008**, *18*, 350–354.
(27) Rao, A. M.; Richter, E.; Bandow, S.; Chase, B.; Eklund, P. C.; Williams, K. A.; Fang, S.; Subbaswamy, K. R.; Menon, M.; Thess, A.; Smalley, R. E.; Dresselhaus, G.; Dresselhaus, M. S. *Science* **1997**, *275*, 187–191.
(28) Bandow, S.; Rao, A. M.; Williams, K. A.; Thess, A.; Smalley, R. E.; Eklund, P. C. *J. Phys. Chem. B* **1997**, *101*, 8839–8842.
(29) Bandyopadhyaya, R.; Nativ-Roth, E.; Regev, O.; Yerushalmi-Rozen, R. *Nano Lett.* **2002**, *2*, 25–28.
(30) Nakashima, N.; Tomonari, Y.; Murakami, H. *Chem. Lett.* **2002**, *31*, 638–639.
(31) Zheng, M.; Jagota, A.; Semke, E. D.; Diner, B. A.; Mclean, R. S.; Lustig, S. R.; Richardson, R. E.; Tassi, N. G. *Nat. Mater.* **2003**, *2*, 338–342.
(32) Matarredona, O.; Rhoads, H.; Li, Z.; Harwell, J. H.; Balzano, L.; Resasco, D. E. *J. Phys. Chem. B* **2003**, *107*, 13357–13367.
(33) Wang, D.; Ji, W. X.; Li, Z. C.; Chen, L. *J. Am. Chem. Soc.* **2006**, *128*, 6556–6557.
(34) Novoselov, K. S.; Geim, A. K.; Morozov, S. V.; Jiang, D.; Zhang, Y.; Dubonos, S. V.; Grigorieva, I. V.; Firsov, A. A. *Science* **2004**, *306*, 666–669.
(35) Zhang, Y. B.; Tan, Y. W.; Stormer, H. L.; Kim, P. *Nature* **2005**, *438*, 201–204.
(36) Gomez-Navarro, C.; Weitz, R. T.; Bittner, A. M.; Scolari, M.; Mews, A.; Burghard, M.; Kern, K. *Nano Lett.* **2007**, *7*, 3499–3503.
(37) Rutter, G. M.; Crain, J. N.; Guisinger, N. P.; Li, T.; First, P. N.; Stroscio, J. A. *Science* **2007**, *317*, 219–222.
(38) Oostinga, J. B.; Heersche, H. B.; Liu, X. L.; Morpurgo, A. F.; Vandersypen, L. M. K. *Nat. Mater.* **2008**, *7*, 151–157.
(39) Balandin, A. A.; Ghosh, S.; Bao, W. Z.; Calizo, I.; Teweldebrhan, D.; Miao, F.; Lau, N. *Nano Lett.* **2008**, *8*, 902–907.
(40) Dikin, D. A.; Stankovich, S.; Zimney, E. J.; Piner, R. D.; Dommett, G. H. B.; Evmenenko, G.; Nguyen, S. T.; Ruoff, R. S. *Nature* **2007**, *448*, 457–460.
(41) Park, S.; Lee, K. S.; Bozoklu, G.; Cai, W.; Nguyen, S. T.; Ruoff, R. S. *ACS Nano* **2008**, *2*, 572–578.
(42) Stankovich, S.; Dikin, D. A.; Dommett, G. H. B.; Kohlhaas, K. M.; Zimney, E. J.; Stach, E. A.; Piner, R. D.; Nguyen, S. T.; Ruoff, R. S. *Nature* **2006**, *442*, 282–286.
(43) Geim, A. K.; Novoselov, K. S. *Nat. Mater.* **2007**, *6*, 183–191.
(44) Hirata, M.; Gotou, T.; Horiuchi, S.; Fujiwara, M.; Ohba, M. *Carbon* **2004**, *42*, 2929–2937.
(45) Titelman, G. I.; Gelman, V.; Bron, S.; Khalfin, R. L.; Cohen, Y.; Bianco-Peled, H. *Carbon* **2005**, *43*, 641–649.
(46) Szabo, T.; Tombacz, E.; Illes, E.; Dekany, I. *Carbon* **2006**, *44*, 537–545.
(47) Guldi, D. M.; Rahman, G. M. A.; Jux, N.; Balbinot, D.; Hartnagel, U.; Tagmatarchis, N.; Prato, M. *J. Am. Chem. Soc.* **2005**, *127*, 9830–9838.
(48) Ikeda, A.; Nobusawa, K.; Hamano, T.; Kikuchi, J. *Org. Lett.* **2006**, *8*, 5489–5492.
(49) Cheng, F.; Imin, P.; Maunders, C.; Botton, G.; Adronov, A. *Macromolecules* **2008**, *41*, 2304–2308.
(50) Li, Q.; Li, Z.; Chen, M.; Fang, Y. *Nano Lett.* **2009**, *9*, 2129–2132.
(51) Peigney, A.; Laurent, C.; Flahaut, E.; Bacsa, R. R.; Rousset, A. *Carbon* **2001**, *39*, 507–514.

JP103745G